Physics Letters B 759 (2016) 282–292

Contents lists available at ScienceDirect

Physics Letters B

www.elsevier.com/locate/physletb

Observation of the $\Lambda_b^0 \to \Lambda\phi$ decay

The LHCb Collaboration

ARTICLE INFO

Article history:
Received 10 March 2016
Received in revised form 13 May 2016
Accepted 24 May 2016
Available online 26 May 2016
Editor: W.-D. Schlatter

ABSTRACT

The $\Lambda_b^0 \to \Lambda\phi$ decay is observed using data corresponding to an integrated luminosity of 3.0 fb^{-1} recorded by the LHCb experiment. The decay proceeds at leading order via a $b \to s\bar{s}s$ loop transition and is therefore sensitive to the possible presence of particles beyond the Standard Model. A first observation is reported with a significance of 5.9 standard deviations. The value of the branching fraction is measured to be $(5.18 \pm 1.04 \pm 0.35\,^{+0.67}_{-0.62}) \times 10^{-6}$, where the first uncertainty is statistical, the second is systematic, and the third is related to external inputs. Triple-product asymmetries are measured to be consistent with zero.

© 2016 The Author. Published by Elsevier B.V. This is an open access article under the CC BY license (http://creativecommons.org/licenses/by/4.0/). Funded by SCOAP^3.

1. Introduction

In the Standard Model (SM), the flavour-changing neutral current decay $\Lambda_b^0 \to \Lambda\phi$ proceeds via a $b \to s\bar{s}s$ loop (penguin) process. A Feynman diagram of the gluonic penguin that contributes to this decay at leading order is displayed in Fig. 1. This transition has been the subject of theoretical and experimental interest in B_s^0 and B^0 decays, since possible beyond the SM particles in the loop could induce non-SM *CP* violation [1–3]. The process has been probed with decay-time-dependent methods in the $B_s^0 \to \phi\phi$ and $B^0 \to K_S^0\phi$ decay modes [4–7], which test for *CP* violation in the interference between mixing and decay. In addition, measurements of *CP* violation in the decay have been performed with the flavour-specific $B^0 \to K^{*0}\phi$ channel [8]. The results to date are consistent with *CP* conservation in the $b \to s\bar{s}s$ process. Model-independently, non-SM physics contributions could appear differently in these decay modes, though many models contain strong correlations [9].

Measurements with Λ_b^0 baryons offer the possibility to look for *CP* violation in the decay, both by studying *CP* asymmetries and by means of *T*-odd observables. These observables have been studied in greater detail for B_s^0 and B^0 meson decays than those for Λ_b^0 baryons [4,8,10,11]. Proposed methods to study *T*-odd asymmetries of Λ_b^0 baryons [12] exploit the polarisation structure of $\Lambda_b^0 \to \Lambda V$ decays, where V denotes a vector resonance [12], and can be affected by the initial Λ_b^0 polarisation if non-zero. An LHCb measurement of the initial polarisation in $\Lambda_b^0 \to J/\psi\Lambda$ decays has yielded a value consistent with zero, though polarisation at the level of 10% is possible given statistical uncertainties [13]. No SM prediction exists specifically for the *T*-odd asymmetries in $\Lambda_b^0 \to \Lambda\phi$ decays, though no large asymmetries are expected given the prediction of *CP* conservation in the decays of beauty mesons for the same transition. Measurements of *CP* asymmetries have been performed by LHCb in an inclusive analysis of $\Lambda_b^0 \to \Lambda hh'$ decays [14], where $h(h')$ refers to a kaon or pion, with corresponding *CP* asymmetries measured to be consistent with zero.

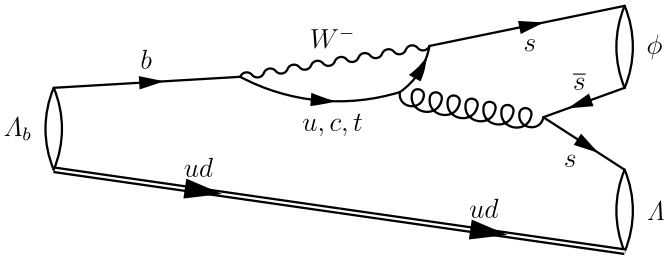

Fig. 1. Feynman diagram contributing to the $\Lambda_b^0 \to \Lambda\phi$ decay.

In this paper, a measurement of the $\Lambda_b^0 \to \Lambda\phi$ branching fraction is presented using the $B^0 \to K_S^0\phi$ decay as a normalisation channel, which has a measured branching fraction of $(7.3^{+0.7}_{-0.6}) \times 10^{-6}$ [15]. The selection requirements used to isolate the $\Lambda_b^0 \to \Lambda\phi$ decay with well-understood efficiencies reject suitable control channels for a ΔA_{CP} measurement. The $\Lambda_b^0 \to \Lambda\phi$ sample is then used to perform measurements of the *T*-odd triple-product asymmetries, which do not require a control channel. The results are based on *pp* collision data corresponding to an integrated luminosity of 1.0 fb^{-1} and 2.0 fb^{-1} collected by the LHCb experiment at centre-of-mass energies of $\sqrt{s} = 7$ TeV in 2011 and 8 TeV in 2012, respectively.

2. Detector and simulation

The LHCb detector [16,17] is a single-arm forward spectrometer covering the pseudorapidity range $2 < \eta < 5$, designed for the

http://dx.doi.org/10.1016/j.physletb.2016.05.077
0370-2693/© 2016 The Author. Published by Elsevier B.V. This is an open access article under the CC BY license (http://creativecommons.org/licenses/by/4.0/). Funded by SCOAP^3.

study of particles containing b or c quarks. The detector includes a high-precision tracking system consisting of a silicon-strip vertex detector surrounding the pp interaction region, a large-area silicon-strip detector located upstream of a dipole magnet with a bending power of about 4 Tm, and three stations of silicon-strip detectors and straw drift tubes placed downstream of the magnet. The tracking system provides a measurement of momentum, p, of charged particles with a relative uncertainty that varies from 0.5% at low momentum to 1.0% at 200 GeV/c. The minimum distance of a track to a primary vertex, the impact parameter, is measured with a resolution of $(15 + 29/p_{\rm T})$ μm, where $p_{\rm T}$ is the component of the momentum transverse to the beam, in GeV/c. Different types of charged hadrons are distinguished using information from two ring-imaging Cherenkov detectors. Photons, electrons and hadrons are identified by a calorimeter system consisting of scintillating-pad and preshower detectors, an electromagnetic calorimeter and a hadronic calorimeter. The online event selection is performed by a trigger, which consists of a hardware stage, based on information from the calorimeter and muon systems, followed by a software stage, which applies a full event reconstruction. At the hardware trigger stage, events are required to have a muon with high $p_{\rm T}$ or a hadron, photon or electron with high transverse energy in the calorimeters. For hadrons, the transverse energy threshold is 3.5 GeV. In the subsequent software trigger, at least one charged particle must have a transverse momentum $p_{\rm T} > 1.7$ GeV/c and be inconsistent with originating from a PV. Finally, the tracks of two or more of the final-state particles are required to form a vertex that is significantly displaced from the PVs. The final state particles that are identified as kaons are required to have a combined invariant mass consistent with that of the ϕ meson.

In the simulation, pp collisions are generated using Pythia8 [18] with a specific LHCb configuration [19]. Decays of hadronic particles are described by EvtGen [20], in which final-state radiation is generated using Photos [21]. The interaction of the generated particles with the detector, and its response, are implemented using the Geant4 toolkit [22] as described in Ref. [23]. The decays of Λ_b^0 baryons are modelled according to a phase-space description. Differences in the efficiencies of protons and anti-protons, at the sub-percent level, are accounted for with the Geant4 implementation of the detector description.

3. Selection

The $\Lambda_b^0 \to \Lambda\phi$ and $B^0 \to K_S^0\phi$ decays are reconstructed through the $\Lambda \to p\pi^-$, $K_S^0 \to \pi^+\pi^-$ and $\phi \to K^+K^-$ final states, where the inclusion of charge conjugate processes is implied throughout the paper. Decays of $\Lambda \to p\pi^-$ and $K_S^0 \to \pi^+\pi^-$ are reconstructed in two different categories. The first category contains Λ (K_S^0) hadrons that decay inside the vertex detector acceptance and the second contains Λ (K_S^0) hadrons that decay outside. These categories are referred to as *long* and *downstream*, respectively. The high resolution of the vertex detector leads to enhanced momentum, vertex, and mass resolutions for candidates in the long category relative to downstream candidates.

Boosted decision trees (BDTs) [24,25] are used to separate signal from background. Different BDTs are trained for decays where the daughter tracks of the Λ (K_S^0) hadron are classified as long or downstream and according to whether the data was collected in 2011 (7 TeV) or 2012 (8 TeV), yielding eight separate BDTs in total. The set of input variables used to train the $\Lambda_b^0 \to \Lambda\phi$ ($B^0 \to K_S^0\phi$) BDTs consists of the Λ_b^0 (B^0) vertex fit quality, $p_{\rm T}$, η, the difference in χ^2 of the PV reconstructed with and without the candidate ($\chi^2_{\rm IP}$), the flight distance squared divided by the associated variance ($\chi^2_{\rm FD}$), the angle between the momentum vector and the vector from the PV to the decay vertex, the Λ (K_S^0) vertex fit quality, and the $p_{\rm T}$ and η of the ϕ and the Λ (K_S^0) hadrons. The minimum and maximum values of the $p_{\rm T}$ and η associated to the final state particles are also included. In addition, the BDT trained on the long category uses the $\chi^2_{\rm IP}$ and $\chi^2_{\rm FD}$ of the Λ (K_S^0) with respect to the associated PV. A PV is reconstructed by requiring a minimum of five good quality tracks that are consistent with originating from the same location within the luminous region. Before the BDTs are trained, initial loose requirements are imposed on the input variables. The BDTs are trained using simulated candidates for the signal and data sidebands for the background. For the training samples, the signal region is defined as being within 150 MeV/c^2 of the known Λ_b^0 (B^0) mass [26]. In addition, the K^+K^- invariant mass is required to be within 20 MeV/c^2 of the known ϕ mass and the $p\pi^-$ invariant mass is required to be within 15 MeV/c^2 of the known Λ mass [26]. The sidebands are defined to be within 500 MeV/c^2 of the known Λ_b^0 (B^0) mass excluding the signal region.

The figure of merit used to determine the requirement imposed on the $\Lambda_b^0 \to \Lambda\phi$ BDT output is defined as $\varepsilon/(3/2 + \sqrt{N_{\rm bkg}})$ [27], where ε is the signal efficiency, and $N_{\rm bkg}$ is the number of background events. This figure of merit is optimised for detection at three standard deviations of decay modes not previously observed. The signal efficiency is obtained from simulated signal candidates and the number of background events is calculated from fits to the data sidebands interpolated to the signal region. This optimisation procedure is performed separately for each BDT.

In contrast to the $\Lambda_b^0 \to \Lambda\phi$ BDTs, the optimum response requirement for the $B^0 \to K_S^0\phi$ BDTs is chosen based on a figure of merit defined as $N_{\rm sig}/\sqrt{N_{\rm sig} + N_{\rm bkg}}$, where $N_{\rm sig}$ is the number of signal events, estimated from the BDT efficiency on simulated datasets normalised using the known branching fraction of the $B^0 \to K_S^0\phi$ decay [15], and $N_{\rm bkg}$ is the expected number of background candidates in the signal region, extrapolated from the B^0 sidebands. This figure of merit is chosen as the $B^0 \to K_S^0\phi$ branching fraction is well measured and is optimised separately for each classifier.

4. Mass fit model

For both the $\Lambda_b^0 \to \Lambda\phi$ and $B^0 \to K_S^0\phi$ decay modes, a three-dimensional fit is employed to determine the signal candidate yields. In the $\Lambda_b^0 \to \Lambda\phi$ case, the three dimensions are the $p\pi^-K^+K^-$, $p\pi^-$, and K^+K^- invariant masses, while in the fit to determine the $B^0 \to K_S^0\phi$ candidate yield, the three dimensions are the $\pi^+\pi^-K^+K^-$, $\pi^+\pi^-$, and K^+K^- invariant masses.

Four components are present in the $B^0 \to K_S^0\phi$ mass fit: the signal $B^0 \to K_S^0\phi$ component, the $B^0 \to K_S^0K^+K^-$ non-resonant contribution, a $\pi^+\pi^-K^+K^-$ combinatorial component, along with a true K_S^0 component combined with two random kaons. The $B^0 \to K_S^0K^+K^-$ non-resonant component has been observed by the BaBar [28], Belle [6] and LHCb [29] Collaborations. This is separated from the signal decay through the different K^+K^- invariant mass line shapes. No significant partially reconstructed background, in which one or more of the final state particles are missed, is found in the B^0 mass region. Peaking backgrounds, from decays in which at least one of the final state particles has been misidentified, are suppressed by the narrow K^+K^- mass window around the ϕ meson and are treated as systematic uncertainties.

The B^0 signal is modelled with the same modified Gaussian function as used in Ref. [30]. The modified Gaussian gives extra degrees of freedom to accommodate extended tails far from the mean. The ϕ signal is modelled with a relativistic Breit–Wigner

shape [31] convolved with a Gaussian resolution function. The K^0_S signal is parametrised by the sum of two Gaussian functions with a common mean. Decays from real B^0 mesons to the $K^0_S K^+K^-$ final state in which the K^+K^- pair is non-resonant are described by the same B^0 and K^0_S line shapes as the signal, but with a phase-space factor to describe the non-resonant kaon pairs. The phase-space factor is given by the expression $(m^2-(2m_K)^2)/m^2$, where m is the K^+K^- invariant mass and m_K is fixed to the value of the charged kaon mass. The use of a Flatté function [32] rather than a phase-space factor to describe a possible scalar component under the ϕ resonance is found to have a negligible effect on the results and is therefore not included. The combinatorial background is modelled by exponential functions in all three mass dimensions.

A simultaneous fit to the long and downstream datasets is performed. The B^0 resolution, modified Gaussian tail parameters and resolutions and fractions of the K^0_S Gaussian functions are constrained to values obtained from a fit to simulated data, performed separately for long and downstream datasets. The total yield and fraction in the downstream dataset are left as free parameters for each component.

The fit to the $\Lambda^0_b \to \Lambda\phi$ channel uses the same fit model as the $B^0 \to K^0_S\phi$ control channel: a modified Gaussian function is used to describe the Λ^0_b mass shape, a double Gaussian model to describe the Λ shape, and a relativistic Breit–Wigner convolved with a Gaussian resolution function to describe that of the ϕ resonance. Due to the relatively unexplored mass spectra present in the $\Lambda^0_b \to \Lambda\phi$ decay, the background contributions have been identified using the data sidebands. In the final fit, four components are present. These are the signal $\Lambda^0_b \to \Lambda\phi$ component, the $\Lambda^0_b \to \Lambda K^+K^-$ non-resonant component in which the K^+K^- dimension is described using the phase-space factor defined previously, combinatorial components with true ϕ or Λ resonances, and a component that has a combinatorial origin in all three mass dimensions. Combinatorial backgrounds are modelled by exponential functions in each fit dimension. As for the case of the $B^0 \to K^0_S\phi$ fit, the total yield and fraction in the downstream dataset are left as free parameters for each component. In addition, the same parameters are constrained to simulated data as in the $B^0 \to K^0_S\phi$ fit.

5. Branching fraction measurement

The $\Lambda^0_b \to \Lambda\phi$ branching fraction is obtained from the relation

$$\mathcal{B}(\Lambda^0_b \to \Lambda\phi) = \frac{\epsilon^{\rm tot}_{B^0\to K^0_S\phi}}{\epsilon^{\rm tot}_{\Lambda^0_b\to\Lambda\phi}} \cdot \frac{f_d}{f_{\Lambda^0_b}} \cdot \frac{N_{\Lambda^0_b\to\Lambda\phi}}{N_{B^0\to K^0_S\phi}} \cdot \frac{\mathcal{B}(B^0\to K^0\phi)}{2} \cdot \frac{\mathcal{B}(K^0_S\to\pi^+\pi^-)}{\mathcal{B}(\Lambda\to p\pi^-)}, \quad (1)$$

where $\epsilon^{\rm tot}$ denotes the combined efficiency of the candidate reconstruction, the offline selection, the trigger requirements, and the efficiency of detector acceptance; $f_{d(\Lambda^0_b)}$ denotes the fraction of b quarks that hadronise to B^0 (Λ^0_b) hadrons. The ratio is taken from the LHCb measured value $f_{\Lambda^0_b}/f_d = 0.387 \pm 0.033$ [33]. The extra factor 1/2 in Eq. (1) accounts for the fact that only half of K^0 mesons will decay as K^0_S mesons. The value of the $B^0 \to K^0\phi$ branching fraction is taken to be $(7.3^{+0.7}_{-0.6}) \times 10^{-6}$ [15], while the PDG values of the Λ and K^0_S branching fractions are used [26].

The reconstruction, selection and software trigger efficiencies, as well as the acceptance of the LHCb detector, are determined from simulated samples, using data-driven correction factors where necessary. The different interaction cross-sections of the final-state particles with the detector material are accounted for using simulated datasets.

For the case of the hardware trigger, the efficiency of events triggered by the signal candidate is determined from control samples of $D^0 \to K^-\pi^+$ and $\Lambda \to p\pi^-$ decays. The efficiency of events triggered independently of the signal candidate is determined from simulation. The agreement between data and simulation for the distributions of the variables used in the BDT is verified with the $B^0 \to K^0_S\phi$ data.

Data-driven corrections for the reconstruction efficiency of tracks corresponding to the long category are obtained from J/ψ samples using a tag-and-probe method [34]. This is applied after a separate weighting to ensure agreement in detector occupancy between data and simulation. For measurements of the relative branching fraction of $\Lambda^0_b \to \Lambda\phi$ to $B^0 \to K^0_S\phi$, the final state differs by substituting the proton from the decay of the Λ with a pion. However, due to the differences in the kinematics of the pions from the Λ and the K^0_S decays, the distinct correction factors for both daughters of the Λ and K^0_S are considered. In addition to the track reconstruction efficiency, the vertexing efficiency of long-lived particles contains disagreement between data and simulation. The corresponding correction factors for the long and downstream datasets are determined separately from $D^0 \to \phi K^0_S$ decays.

The yields of the $\Lambda^0_b \to \Lambda\phi$ signal and $B^0 \to K^0_S\phi$ control mode are determined from simultaneous extended unbinned maximum likelihood fits to the respective datasets divided according to the data-taking period and also according to whether the Λ (K^0_S) decay products are reconstructed as long or downstream tracks. Efficiencies are applied to each dataset individually. The projections of the fit result to $\Lambda^0_b \to \Lambda\phi$ data are shown in Fig. 2. The fitted yields are 350 ± 24 and 89 ± 13 for the $B^0 \to K^0_S\phi$ and $\Lambda^0_b \to \Lambda\phi$ decay modes, respectively. The statistical significance of the $\Lambda^0_b \to \Lambda\phi$ decay, determined according to Wilks' theorem [35] from the difference in the likelihood value of the fits with and without the $\Lambda^0_b \to \Lambda\phi$ component, is found to be 6.5 standard deviations. With the systematic uncertainties discussed below included, the significance of the observed $\Lambda^0_b \to \Lambda\phi$ decay yield is calculated to be 5.9 standard deviations. The projections of the fit result to the $B^0 \to K^0_S\phi$ data are shown in Fig. 3. The fit is found to describe the data well in all three dimensions and a clear peak from the control mode is seen.

The systematic contributions to the branching fraction uncertainty budget are summarised in Table 1. The largest contributions to the systematic uncertainties result from data-driven corrections applied to simulated data along with the mass model used to determine the signal yields.

Signal mismodelling is accounted for using a one-dimensional kernel estimate for the description of the simulated mass distributions [36]. Background mismodelling is accounted for using a linear function. The kernel estimate is used in both the signal and control channels to describe the Λ^0_b, B^0, K^0_S, and Λ line shapes. In order to determine the systematic uncertainties, 1000 pseudoexperiments are generated with the alternative model and are subsequently fitted with the nominal model. The average difference between the generated and fitted yield values is taken as the systematic uncertainty. This leads to uncertainties of 3.0% and 0.6% for the signal and control mode yields, respectively.

Systematic uncertainties associated with the efficiency corrections from simulated datasets are considered. The limited size of the simulated sample gives rise to an uncertainty of 2.2%. The main uncertainties in the tracking and vertexing correction factors arise from the limited size of the control sample, which leads to uncertainties of 0.5% and 2.6%, respectively. For the case of the trigger efficiency, uncertainties related to the software trigger cancel between the signal and control modes, as the software trigger decision is made only on the decay products of the ϕ meson. Un-

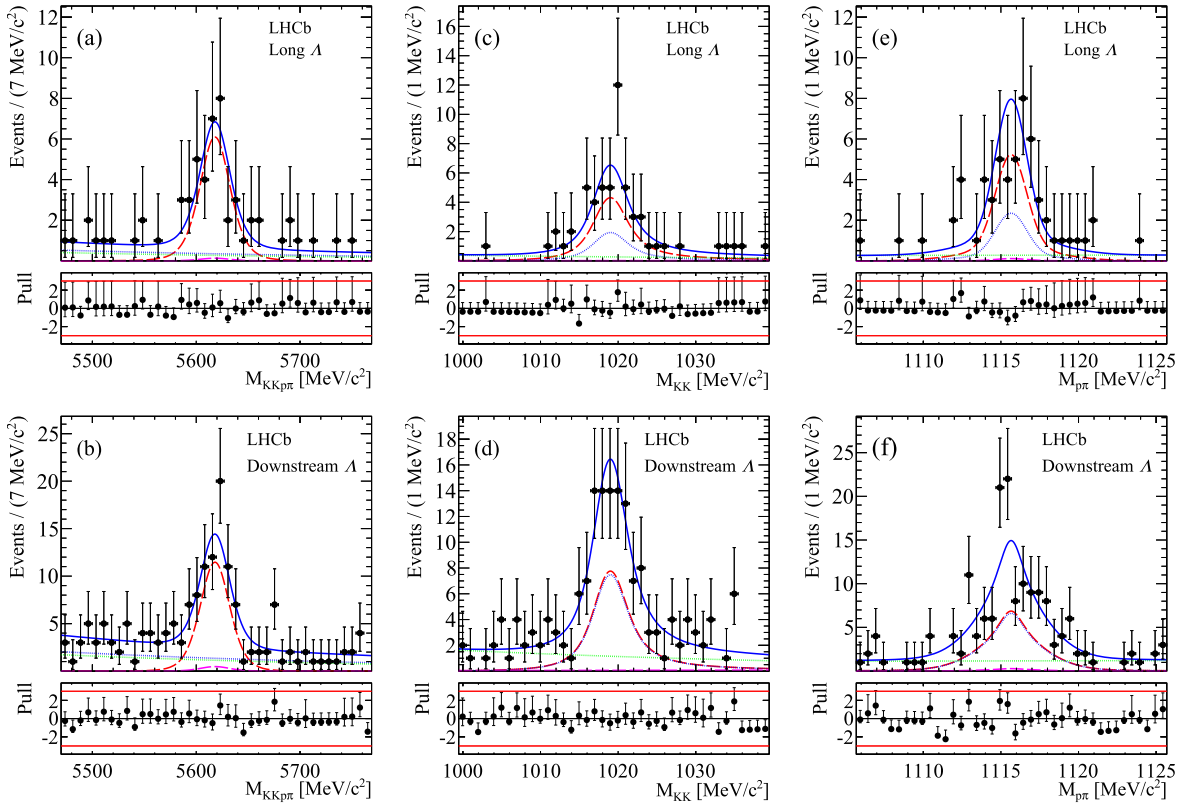

Fig. 2. Fit projections to the $p\pi^-K^+K^-$ invariant mass in the (a) long and (b) downstream datasets, the K^+K^- invariant mass in the (c) long and (d) downstream datasets, and the $p\pi^-$ invariant mass in the (e) long and (f) downstream datasets. The total fit projection is given by the blue solid line. The blue and green dotted lines represent the $\phi + \Lambda$ and pure combinatorial fit components, respectively. The red and magenta dashed lines represent the $\Lambda_b^0 \to \Lambda\phi$ signal and the $\Lambda_b^0 \to \Lambda K^+K^-$ non-resonant components, respectively. Black points represent the data. Data uncertainties are Poisson 68% confidence intervals. (For interpretation of the references to colour in this figure legend, the reader is referred to the web version of this article.)

certainties in the efficiency of the hardware trigger selections are estimated using data-driven methods, for which an uncertainty of 2.8% is applied. The BDTs used to select signal and control modes use the same input variables. Biases could exist if the simulation mismodels these variables differently for signal and control modes. In order to quantify this effect, the control mode is selected with the same classifier as the signal decay. The difference in the measured branching fraction is found to be 4.1%.

The $\Lambda_b^0 \to \Sigma^0(\to \Lambda\gamma)K^+K^-$ and $\Lambda_b^0 \to pK^-\phi$ decay modes are found to be the only significant peaking background contributions. However, for the case of the $\Lambda_b^0 \to pK^-\phi$ decay, the resulting candidates are reconstructed in the long dataset only. With the assumption that the branching fraction for this decay is the same size as for the signal, the contribution is $< 1\%$ compared to the $\Lambda_b^0 \to \Lambda\phi$ decay and far from the Λ_b^0 signal region, and is therefore ignored. In order to determine the shape in the $p\pi^-K^+K^-$ spectrum of the $\Lambda_b^0 \to \Sigma^0K^+K^-$ decay, a sample of $\Lambda_b^0 \to \Sigma^0K^+K^-$ simulated events is used with a requirement that the K^+K^- invariant mass is within 30 MeV/c^2 of the nominal ϕ mass. The inclusion of an additional fit component using the shape from simulation is found to have a small effect on the signal yield at the level of 0.1%, which is assigned as a systematic uncertainty. For the case of the $B^0 \to K_S^0\phi$ control mode, no peaking background contributions have been identified.

The branching fraction ratio is measured to be

$$\frac{\mathcal{B}(\Lambda_b^0 \to \Lambda\phi)}{\mathcal{B}(B^0 \to K_S^0\phi)} \frac{f_{\Lambda_b^0}}{f_{B^0}} = 0.55 \pm 0.11\,(\text{stat}) \pm 0.04\,(\text{syst}).$$

The use of the world average value of $\mathcal{B}(B^0 \to K_S^0\phi) = (3.65^{+0.35}_{-0.30}) \times 10^{-6}$ [15] gives the final result of

$$\begin{aligned}\mathcal{B}(\Lambda_b^0 \to \Lambda\phi)/10^{-6} = 5.18 &\pm 1.04\,(\text{stat}) \\ &\pm 0.35\,(\text{syst})^{+0.50}_{-0.43}\,(\mathcal{B}(B^0 \to K_S^0\phi)) \\ &\pm 0.44\,(f_d/f_{\Lambda_b^0}).\end{aligned}$$

6. Triple-product asymmetries

The $\Lambda_b^0 \to \Lambda\phi$ decay is a spin-1/2 to spin-1/2 plus vector transition. Five angles are needed to describe this decay since Λ_b^0 baryons may potentially be produced with a transverse polarisation in proton–proton collisions [13], as shown in Fig. 4. The angle θ is defined as the polar angle of the Λ baryon in the Λ_b^0 rest frame with respect to the normal vector defined through

$$\hat{n} = \frac{\vec{p}_1 \times \vec{p}_{\Lambda_b^0}}{|\vec{p}_1 \times \vec{p}_{\Lambda_b^0}|}, \tag{2}$$

where $\vec{p}_1$ is the momentum of an incoming proton and $\vec{p}_{\Lambda_b^0}$ is the momentum of the Λ_b^0 baryon. The angles θ_Λ and Φ_Λ are defined as the polar and azimuthal angles of the proton from the decay of the Λ baryon in the Λ rest frame. The angles θ_ϕ and Φ_ϕ are defined as the polar and azimuthal angles of the K^+ meson in the rest frame of the ϕ meson.

Triple-product asymmetries, which are odd under time-reversal, have been proposed by Leitner and Ajaltouni using the azimuthal angles Φ_{n_i}, $i \in \{\Lambda, \phi\}$, defined as [12]

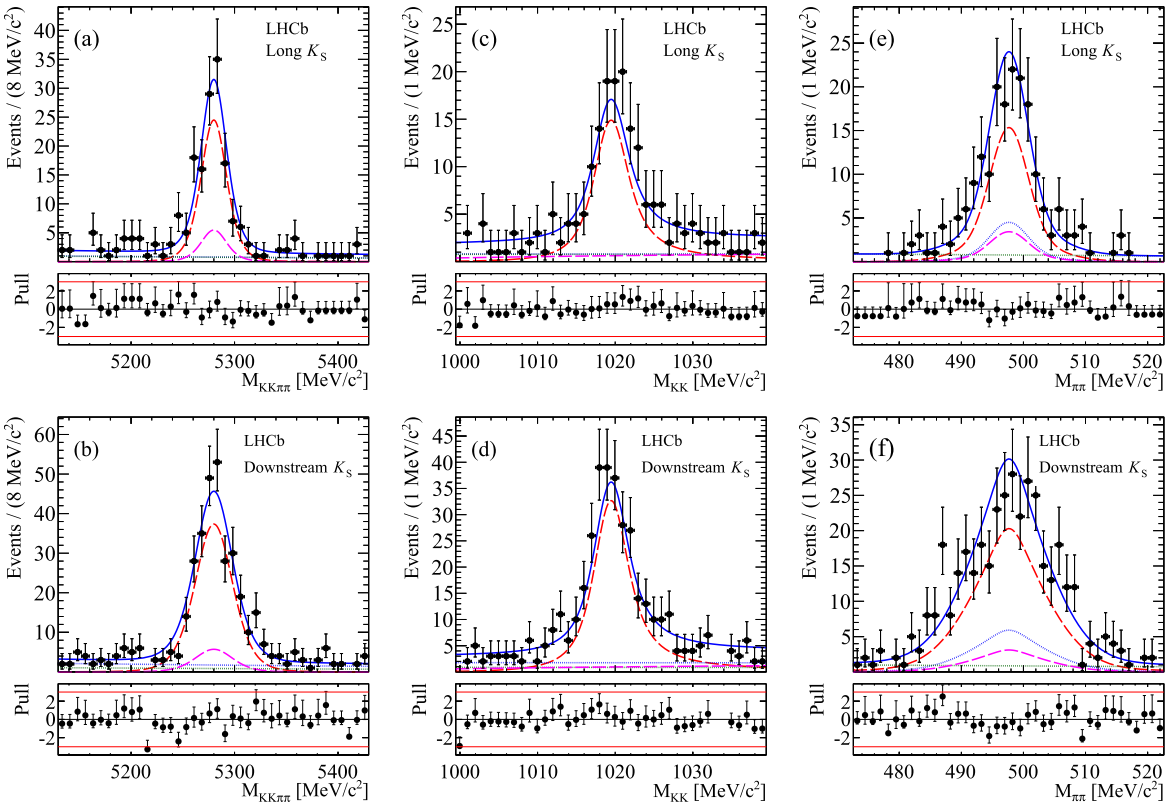

Fig. 3. Fit projections to the $\pi^+\pi^-K^+K^-$ invariant mass in the (a) long and (b) downstream datasets, the K^+K^- invariant mass in the (c) long and (d) downstream datasets, and the $\pi^+\pi^-$ invariant mass in the (e) long and (f) downstream datasets. The total fit projection is given by the blue solid line. The green and blue dotted lines represent the combinatorial and K^0_S + random K^+K^- fit components, respectively. The red and magenta dashed lines represent the $B^0 \to K^0_S\phi$ signal and the $B^0 \to K^0_S K^+K^-$ non-resonant components, respectively. Black points represent the data. Data uncertainties are Poisson 68% confidence intervals. (For interpretation of the references to colour in this figure legend, the reader is referred to the web version of this article.)

Table 1
Systematic uncertainty contributions to the branching fraction ratio.

Source	Uncertainty (%)
Mass model	3.0
Simulation sample size	2.2
Tracking efficiency	0.5
Vertex efficiency	2.6
Hardware trigger	2.8
Selection efficiency	4.1
Peaking background	0.1
Total	6.7

$$\cos\Phi_{n_i} = \vec{e}_Y \cdot \vec{u}_i, \tag{3}$$

$$\sin\Phi_{n_i} = \vec{e}_Z \cdot (\vec{e}_Y \times \vec{u}_i), \tag{4}$$

where

$$\vec{u}_i = \frac{\vec{e}_Z \times \hat{n}_i}{|\vec{e}_Z \times \hat{n}_i|}. \tag{5}$$

The basis $\{\vec{e}_X, \vec{e}_Y, \vec{e}_Z\}$ is defined in the Λ_b^0 rest frame, in which $\vec{e}_Z$ is parallel to $\hat{n}$, $\vec{e}_X$ is chosen to be parallel to the momentum of the incoming proton, and $\hat{n}_{\Lambda(\phi)}$ is the normal vector to the $\Lambda(\phi)$ decay plane, defined through

$$\hat{n}_\Lambda = \frac{\vec{p}_p \times \vec{p}_\pi}{|\vec{p}_p \times \vec{p}_\pi|}, \tag{6}$$

$$\hat{n}_\phi = \frac{\vec{p}_{K^+} \times \vec{p}_{K^-}}{|\vec{p}_{K^+} \times \vec{p}_{K^-}|}. \tag{7}$$

Asymmetries in $\cos\Phi_{n_i}$ and $\sin\Phi_{n_i}$, where $i \in \{\Lambda, \phi\}$, are defined as

$$A_i^c = \frac{N_i^{+,c} - N_i^{-,c}}{N_i^{+,c} + N_i^{-,c}}, \tag{8}$$

$$A_i^s = \frac{N_i^{+,s} - N_i^{-,s}}{N_i^{+,s} + N_i^{-,s}}, \tag{9}$$

where $N_i^{+(-),c}$ and $N_i^{+(-),s}$ denote the number of candidates for which the $\cos\Phi_{n_i}$ and $\sin\Phi_{n_i}$ observables are positive (negative), respectively.

The asymmetries $A_\Lambda^{c,s}$ and $A_\phi^{c,s}$ are determined experimentally through a simultaneous unbinned maximum likelihood fit to datasets in which the relevant observables are positive and negative. The fit construction and observables are identical to that used for the branching fraction measurement. However, the yields for each dataset are parametrised in terms of the total yield, N_j, and the asymmetry, A_j, for fit component j as

$$N_j^+ = \frac{N^j}{2}(1 + A_j), \tag{10}$$

$$N_j^- = \frac{N^j}{2}(1 - A_j). \tag{11}$$

Distributions of the $\sin\Phi_{n_{(\Lambda,\phi)}}$ and $\cos\Phi_{n_{(\Lambda,\phi)}}$ observables from $\Lambda_b^0 \to \Lambda\phi$ data have been extracted using the *sPlot* method [37] and are provided in Fig. 5. The numerical values of the fitted asymmetries are given in Table 2.

Mismodelling of the mass components could lead to background contamination in the determination of the asymmetries. In

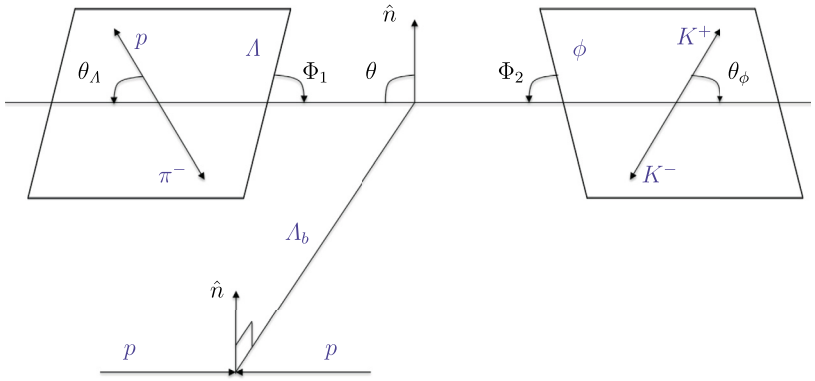

Fig. 4. Decay angles for the $\Lambda_b^0 \to \Lambda\phi$ decay, where the angles are defined in the text.

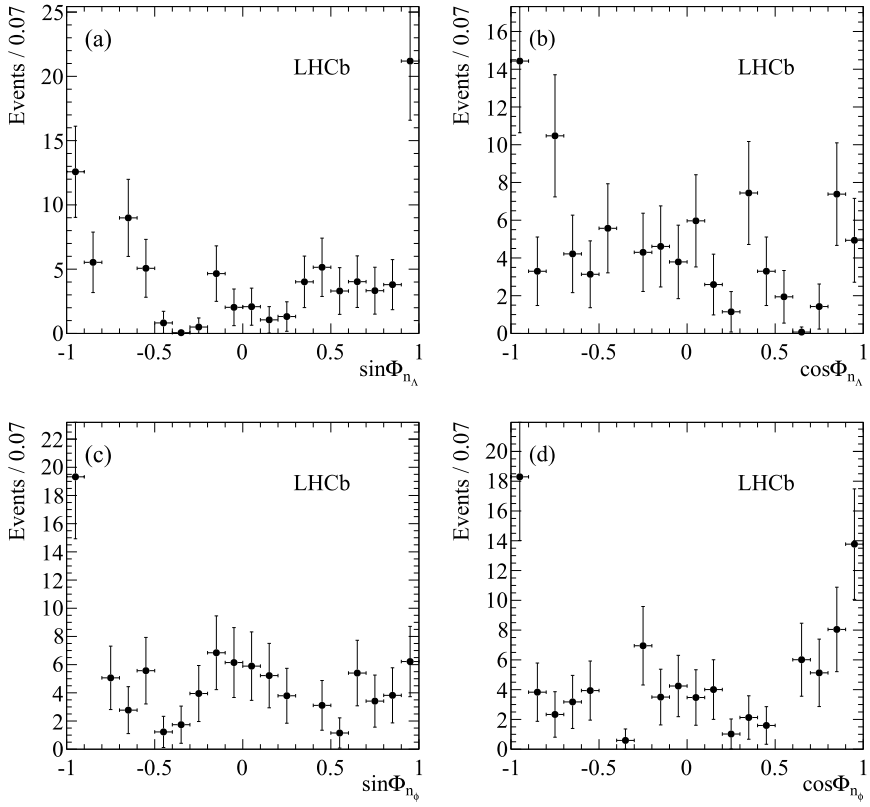

Fig. 5. Distributions of the angular observables: (a) $\sin\Phi_{n_\Lambda}$, (b) $\cos\Phi_{n_\Lambda}$, (c) $\sin\Phi_{n_\phi}$, (d) $\cos\Phi_{n_\phi}$ from weighted $\Lambda_b^0 \to \Lambda\phi$ data.

Table 2
Asymmetries measured from $\Lambda_b^0 \to \Lambda\phi$ data events.

Asymmetry	Fit value
A_Λ^c	-0.22 ± 0.12
A_Λ^s	0.13 ± 0.12
A_ϕ^c	-0.01 ± 0.12
A_ϕ^s	-0.07 ± 0.12

the determination of the uncertainty related to the mass model, two contributions are considered. These are the line shape models and the background asymmetries. The effects of the line shapes are quantified using the same method as the branching fraction measurement, *i.e.* the generation of datasets with a one-dimensional kernel estimate of the simulation mass distributions in addition to modification of the background description. In the nominal fit, components that are not from the $\Lambda_b^0 \to \Lambda\phi$ signal have zero asymmetries. For background components this is justified due to the uncorrelated kinematics of the K^+K^- and $p\pi^-$ systems. However, the non-resonant $\Lambda_b^0 \to \Lambda K^+K^-$ contribution could have non-zero asymmetries. The systematic uncertainty due to the assumption of zero background asymmetries is determined through comparing the nominal fit against the fit with all possible asymmetries allowed to vary freely.

Efficiencies are found to be independent of the $\sin\Phi_{n_i}$ and $\cos\Phi_{n_i}$ observables. The systematic uncertainty due to the angular acceptance is then taken from the statistical uncertainty in fits to the simulated datasets, after the application of an appropriate weighting to account for the differences between data and simulation. The resolutions of the angular observables are found from simulated events to be 32.3 mrad and 22.1 mrad for the Φ_{n_Λ} and Φ_{n_ϕ} angles, respectively. The uncertainty due to bin migration is then assigned assuming maximal asymmetry and leads to minor uncertainties of 0.007 for the Φ_{n_ϕ} angle and 0.010 for the Φ_{n_Λ}

Table 3
Systematic uncertainty contributions to the triple-product asymmetries.

Source	A_Λ^c	A_Λ^s	A_ϕ^c	A_ϕ^s
Mass model	0.061	0.051	0.026	0.009
Angular acceptance	0.010	0.010	0.010	0.010
Angular resolution	0.008	0.008	0.005	0.005
Total	0.062	0.053	0.028	0.014

angle. Systematic contributions to the triple-product uncertainty budget are summarised in Table 3.

7. Summary

A search for the $\Lambda_b^0 \to \Lambda\phi$ decay is presented based on a dataset of 3.0 fb^{-1} collected by the LHCb experiment in 2011 and 2012. The decay is observed for the first time with a significance of 5.9 standard deviations including systematic uncertainties. The branching fraction is found to be

$$\begin{aligned}\mathcal{B}(\Lambda_b^0 \to \Lambda\phi)/10^{-6} = 5.18 \pm 1.04\,(\text{stat}) \\ \pm 0.35\,(\text{syst})^{+0.50}_{-0.43}\,(\mathcal{B}(B^0 \to K^0_S\phi)) \\ \pm 0.44\,(f_d/f_{\Lambda_b^0}).\end{aligned}$$

Triple-product asymmetries are measured to be

$$\begin{aligned}A_\Lambda^c &= -0.22 \pm 0.12\,(\text{stat}) \pm 0.06\,(\text{syst}),\\ A_\Lambda^s &= 0.13 \pm 0.12\,(\text{stat}) \pm 0.05\,(\text{syst}),\\ A_\phi^c &= -0.01 \pm 0.12\,(\text{stat}) \pm 0.03\,(\text{syst}),\\ A_\phi^s &= -0.07 \pm 0.12\,(\text{stat}) \pm 0.01\,(\text{syst}),\end{aligned}$$

and are consistent with zero. Data collected by the LHCb experiment in the forthcoming years will improve the statistical precision of these measurements and enable the dynamics of $b \to s$ transitions in beauty baryons to be probed in greater detail, which will greatly enhance the reach of searches for physics beyond the SM.

Acknowledgements

We express our gratitude to our colleagues in the CERN accelerator departments for the excellent performance of the LHC. We thank the technical and administrative staff at the LHCb institutes. We acknowledge support from CERN and from the national agencies: CAPES, CNPq, FAPERJ and FINEP (Brazil); NSFC (China); CNRS/IN2P3 (France); BMBF, DFG and MPG (Germany); INFN (Italy); FOM and NWO (The Netherlands); MNiSW and NCN (Poland); MEN/IFA (Romania); MinES and FANO (Russia); MinECo (Spain); SNSF and SER (Switzerland); NASU (Ukraine); STFC (United Kingdom); NSF (USA). We acknowledge the computing resources that are provided by CERN, IN2P3 (France), KIT and DESY (Germany), INFN (Italy), SURF (The Netherlands), PIC (Spain), GridPP (United Kingdom), RRCKI and Yandex LLC (Russia), CSCS (Switzerland), IFIN-HH (Romania), CBPF (Brazil), PL-GRID (Poland) and OSC (USA). We are indebted to the communities behind the multiple open source software packages on which we depend. Individual groups or members have received support from AvH Foundation (Germany), EPLANET, Marie Skłodowska-Curie Actions and ERC (European Union), Conseil Général de Haute-Savoie, Labex ENIGMASS and OCEVU, Région Auvergne (France), RFBR and Yandex LLC (Russia), GVA, XuntaGal and GENCAT (Spain), Herchel Smith Fund, The Royal Society, Royal Commission for the Exhibition of 1851 and the Leverhulme Trust (United Kingdom).

References

[1] Y. Shimizu, M. Tanimoto, K. Yamamoto, Supersymmetry contributions to CP violations in $b \to s$ and $b \to d$ transitions taking account of new data, Phys. Rev. D 87 (2013) 056004, arXiv:1212.6486.
[2] A. Datta, M. Imbeault, D. London, $B \to \phi K^*$, $B \to \phi K_S$ and new physics, Phys. Lett. B 671 (2009) 256, arXiv:0811.2957.
[3] T. Moroi, CP violation in $B^0 \to \phi K_S$ in SUSY GUT with right-handed neutrinos, Phys. Lett. B 493 (2000) 366, arXiv:hep-ph/0007328.
[4] LHCb Collaboration, R. Aaij, et al., Measurement of *CP* violation in $B_s^0 \to \phi\phi$ decays, Phys. Rev. D 90 (2014) 052011, arXiv:1407.2222.
[5] LHCb Collaboration, R. Aaij, et al., First measurement of the *CP*-violating phase in $B_s^0 \to \phi\phi$ decays, Phys. Rev. Lett. 110 (2013) 241802, arXiv:1303.7125.
[6] Belle Collaboration, K. Abe, et al., Measurement of time-dependent CP-violating asymmetries in $B^0 \to \phi K_S^0$, $K^+K^-K_S^0$, and $\eta' K_S^0$ decays, Phys. Rev. Lett. 91 (2003) 261602, arXiv:hep-ex/0308035.
[7] BaBar Collaboration, J.P. Lees, et al., Study of CP violation in Dalitz-plot analyses of $B^0 \to K^+K^-K_S^0$, $B^+ \to K^+K^-K^+$, and $B^+ \to K_S^0K_S^0K^+$, Phys. Rev. D 85 (2012) 112010, arXiv:1201.5897.
[8] LHCb Collaboration, R. Aaij, et al., Measurement of polarization amplitudes and *CP* asymmetries in $B^0 \to \phi K^*(892)^0$, J. High Energy Phys. 05 (2014) 069, arXiv:1403.2888.
[9] M. Raidal, *CP* asymmetry in $B \to \phi K_S$ decays in left-right models and its implications on B_s decays, Phys. Rev. Lett. 89 (2002) 231803, arXiv:hep-ph/0208091.
[10] M. Gronau, J.L. Rosner, Triple product asymmetries in K, $D_{(s)}$ and $B_{(s)}$ decays, Phys. Rev. D 84 (2011) 096013, arXiv:1107.1232.
[11] S.K. Patra, A. Kundu, CPT violation and triple-product correlations in B decays, Phys. Rev. D 87 (11) (2013) 116005, arXiv:1305.1417.
[12] O. Leitner, Z.J. Ajaltouni, Testing CP and time reversal symmetries with $\Lambda_b \to \Lambda V(1-)$ decays, Nucl. Phys. B, Proc. Suppl. 174 (2007) 169, arXiv:hep-ph/0610189.
[13] LHCb Collaboration, R. Aaij, et al., Measurements of the $\Lambda_b^0 \to J/\psi\Lambda$ decay amplitudes and the Λ_b^0 polarisation in pp collisions at $\sqrt{s} = 7$ TeV, Phys. Lett. B 724 (2013) 27, arXiv:1302.5578.
[14] LHCb Collaboration, R. Aaij, et al., Observations of $\Lambda_b^0 \to \Lambda K^+\pi^-$ and $\Lambda_b^0 \to \Lambda K^+K^-$ decays and searches for other Λ_b^0 and Ξ_b^0 decays to Λh^+h^- final states, J. High Energy Phys. (2016), http://dx.doi.org/10.1007/JHEP05(2016)081, arXiv:1603.00413.
[15] Heavy Flavor Averaging Group, Y. Amhis, et al., Averages of b-hadron, c-hadron, and τ-lepton properties as of summer 2014, arXiv:1412.7515, updated results and plots available at http://www.slac.stanford.edu/xorg/hfag/.
[16] LHCb Collaboration, A.A. Alves Jr., et al., The LHCb detector at the LHC, J. Instrum. 3 (2008) S08005.
[17] LHCb Collaboration, R. Aaij, et al., LHCb detector performance, Int. J. Mod. Phys. A 30 (2015) 1530022, arXiv:1412.6352.
[18] T. Sjöstrand, S. Mrenna, P. Skands, PYTHIA 6.4 physics and manual, J. High Energy Phys. 05 (2006) 026, arXiv:hep-ph/0603175;
T. Sjöstrand, S. Mrenna, P. Skands, A brief introduction to PYTHIA 8.1, Comput. Phys. Commun. 178 (2008) 852, arXiv:0710.3820.
[19] I. Belyaev, et al., Handling of the generation of primary events in Gauss, the LHCb simulation framework, J. Phys. Conf. Ser. 331 (2011) 032047.
[20] D.J. Lange, The EvtGen particle decay simulation package, Nucl. Instrum. Methods Phys. Res., Sect. A 462 (2001) 152.
[21] P. Golonka, Z. Was, PHOTOS Monte Carlo: a precision tool for QED corrections in Z and W decays, Eur. Phys. J. C 45 (2006) 97, arXiv:hep-ph/0506026.
[22] Geant4 Collaboration, J. Allison, et al., Geant4 developments and applications, IEEE Trans. Nucl. Sci. 53 (2006) 270;
Geant4 Collaboration, S. Agostinelli, et al., Geant4: a simulation toolkit, Nucl. Instrum. Methods Phys. Res., Sect. A 506 (2003) 250.
[23] M. Clemencic, et al., The LHCb simulation application, Gauss: design, evolution and experience, J. Phys. Conf. Ser. 331 (2011) 032023.
[24] L. Breiman, J.H. Friedman, R.A. Olshen, C.J. Stone, Classification and Regression Trees, Wadsworth international group, Belmont, California, USA, 1984.
[25] R.E. Schapire, Y. Freund, A decision-theoretic generalization of on-line learning and an application to boosting, J. Comput. Syst. Sci. 55 (1997) 119.
[26] Particle Data Group, K.A. Olive, et al., Review of particle physics, Chin. Phys. C 38 (2014) 090001.
[27] G. Punzi, Sensitivity of searches for new signals and its optimization, in: L. Lyons, R. Mount, R. Reitmeyer (Eds.), Statistical Problems in Particle Physics, Astrophysics, and Cosmology, 2003, p. 79, arXiv:physics/0308063.
[28] BaBar Collaboration, B. Aubert, et al., Measurement of CP asymmetries in $B^0 \to \phi K^0$ and $B^0 \to K^+K^-K_S^0$ decays, Phys. Rev. D 71 (2005) 091102, arXiv:hep-ex/0502019.
[29] LHCb Collaboration, R. Aaij, et al., Study of $B_{(s)}^0 \to K_S^0h^+h'^-$ decays with first observation of $B_s^0 \to K_S^0K^\pm\pi^\mp$ and $B_s^0 \to K_S^0\pi^+\pi^-$, J. High Energy Phys. 10 (2013) 143, arXiv:1307.7648.
[30] LHCb Collaboration, R. Aaij, et al., Observation of *CP* violation in $B^\pm \to DK^\pm$ decays, Phys. Lett. B 712 (2012) 203;

LHCb Collaboration, R. Aaij, et al., Observation of CP violation in $B^{\pm} \to DK^{\pm}$ decays, Phys. Lett. B 713 (2012) 351, arXiv:1203.3662 (Erratum).
[31] HERA-B Collaboration, I. Abt, et al., K^{*0} and ϕ meson production in proton–nucleus interactions at $\sqrt{s} = 41.6$ GeV, Eur. Phys. J. C 50 (2007) 315, arXiv:hep-ex/0606049.
[32] S.M. Flatté, On the nature of 0^+ mesons, Phys. Lett. B 63 (1976) 228.
[33] LHCb Collaboration, R. Aaij, et al., Study of the kinematic dependences of Λ_b^0 production in pp collisions and a measurement of the $\Lambda_b^0 \to \Lambda_c^+ \pi^-$ branching fraction, J. High Energy Phys. 08 (2014) 143, arXiv:1405.6842.
[34] LHCb Collaboration, R. Aaij, et al., Measurement of the track reconstruction efficiency at LHCb, J. Instrum. 10 (2015) P02007, arXiv:1408.1251.
[35] S.S. Wilks, The large-sample distribution of the likelihood ratio for testing composite hypotheses, Ann. Math. Stat. 9 (1938) 60.
[36] K.S. Cranmer, Kernel estimation in high-energy physics, Comput. Phys. Commun. 136 (2001) 198, arXiv:hep-ex/0011057.
[37] M. Pivk, F.R. Le Diberder, sPlot: a statistical tool to unfold data distributions, Nucl. Instrum. Methods Phys. Res., Sect. A 555 (2005) 356, arXiv:physics/0402083.

LHCb Collaboration

R. Aaij [39], C. Abellán Beteta [41], B. Adeva [38], M. Adinolfi [47], Z. Ajaltouni [5], S. Akar [6], J. Albrecht [10], F. Alessio [39], M. Alexander [52], S. Ali [42], G. Alkhazov [31], P. Alvarez Cartelle [54], A.A. Alves Jr [58], S. Amato [2], S. Amerio [23], Y. Amhis [7], L. An [3,40], L. Anderlini [18], G. Andreassi [40], M. Andreotti [17,g], J.E. Andrews [59], R.B. Appleby [55], O. Aquines Gutierrez [11], F. Archilli [39], P. d'Argent [12], A. Artamonov [36], M. Artuso [60], E. Aslanides [6], G. Auriemma [26,n], M. Baalouch [5], S. Bachmann [12], J.J. Back [49], A. Badalov [37], C. Baesso [61], S. Baker [54], W. Baldini [17], R.J. Barlow [55], C. Barschel [39], S. Barsuk [7], W. Barter [39], V. Batozskaya [29], V. Battista [40], A. Bay [40], L. Beaucourt [4], J. Beddow [52], F. Bedeschi [24], I. Bediaga [1], L.J. Bel [42], V. Bellee [40], N. Belloli [21,k], I. Belyaev [32], E. Ben-Haim [8], G. Bencivenni [19], S. Benson [39,*], J. Benton [47], A. Berezhnoy [33], R. Bernet [41], A. Bertolin [23], F. Betti [15], M.-O. Bettler [39], M. van Beuzekom [42], S. Bifani [46], P. Billoir [8], T. Bird [55], A. Birnkraut [10], A. Bizzeti [18,i], T. Blake [49], F. Blanc [40], J. Blouw [11], S. Blusk [60], V. Bocci [26], A. Bondar [35], N. Bondar [31,39], W. Bonivento [16], A. Borgheresi [21,k], S. Borghi [55], M. Borisyak [67], M. Borsato [38], M. Boubdir [9], T.J.V. Bowcock [53], E. Bowen [41], C. Bozzi [17,39], S. Braun [12], M. Britsch [12], T. Britton [60], J. Brodzicka [55], E. Buchanan [47], C. Burr [55], A. Bursche [2], J. Buytaert [39], S. Cadeddu [16], R. Calabrese [17,g], M. Calvi [21,k], M. Calvo Gomez [37,p], P. Campana [19], D. Campora Perez [39], L. Capriotti [55], A. Carbone [15,e], G. Carboni [25,l], R. Cardinale [20,j], A. Cardini [16], P. Carniti [21,k], L. Carson [51], K. Carvalho Akiba [2], G. Casse [53], L. Cassina [21,k], L. Castillo Garcia [40], M. Cattaneo [39], Ch. Cauet [10], G. Cavallero [20], R. Cenci [24,t], M. Charles [8], Ph. Charpentier [39], G. Chatzikonstantinidis [46], M. Chefdeville [4], S. Chen [55], S.-F. Cheung [56], M. Chrzaszcz [41,27], X. Cid Vidal [39], G. Ciezarek [42], P.E.L. Clarke [51], M. Clemencic [39], H.V. Cliff [48], J. Closier [39], V. Coco [58], J. Cogan [6], E. Cogneras [5], V. Cogoni [16,f], L. Cojocariu [30], G. Collazuol [23,r], P. Collins [39], A. Comerma-Montells [12], A. Contu [39], A. Cook [47], M. Coombes [47], S. Coquereau [8], G. Corti [39], M. Corvo [17,g], B. Couturier [39], G.A. Cowan [51], D.C. Craik [51], A. Crocombe [49], M. Cruz Torres [61], S. Cunliffe [54], R. Currie [54], C. D'Ambrosio [39], E. Dall'Occo [42], J. Dalseno [47], P.N.Y. David [42], A. Davis [58], O. De Aguiar Francisco [2], K. De Bruyn [6], S. De Capua [55], M. De Cian [12], J.M. De Miranda [1], L. De Paula [2], P. De Simone [19], C.-T. Dean [52], D. Decamp [4], M. Deckenhoff [10], L. Del Buono [8], N. Déléage [4], M. Demmer [10], D. Derkach [67], O. Deschamps [5], F. Dettori [39], B. Dey [22], A. Di Canto [39], F. Di Ruscio [25], H. Dijkstra [39], F. Dordei [39], M. Dorigo [40], A. Dosil Suárez [38], A. Dovbnya [44], K. Dreimanis [53], L. Dufour [42], G. Dujany [55], K. Dungs [39], P. Durante [39], R. Dzhelyadin [36], A. Dziurda [27], A. Dzyuba [31], S. Easo [50,39], U. Egede [54], V. Egorychev [32], S. Eidelman [35], S. Eisenhardt [51], U. Eitschberger [10], R. Ekelhof [10], L. Eklund [52], I. El Rifai [5], Ch. Elsasser [41], S. Ely [60], S. Esen [12], H.M. Evans [48], T. Evans [56], A. Falabella [15], C. Färber [39], N. Farley [46], S. Farry [53], R. Fay [53], D. Fazzini [21,k], D. Ferguson [51], V. Fernandez Albor [38], F. Ferrari [15], F. Ferreira Rodrigues [1], M. Ferro-Luzzi [39], S. Filippov [34], M. Fiore [17,g], M. Fiorini [17,g], M. Firlej [28], C. Fitzpatrick [40], T. Fiutowski [28], F. Fleuret [7,b], K. Fohl [39], M. Fontana [16], F. Fontanelli [20,j], D.C. Forshaw [60], R. Forty [39], M. Frank [39], C. Frei [39], M. Frosini [18], J. Fu [22], E. Furfaro [25,l], A. Gallas Torreira [38], D. Galli [15,e], S. Gallorini [23], S. Gambetta [51], M. Gandelman [2], P. Gandini [56], Y. Gao [3], J. García Pardiñas [38], J. Garra Tico [48], L. Garrido [37], P.J. Garsed [48], D. Gascon [37], C. Gaspar [39], L. Gavardi [10], G. Gazzoni [5], D. Gerick [12], E. Gersabeck [12], M. Gersabeck [55], T. Gershon [49], Ph. Ghez [4], S. Gianì [40], V. Gibson [48], O.G. Girard [40], L. Giubega [30], V.V. Gligorov [39], C. Göbel [61], D. Golubkov [32], A. Golutvin [54,39], A. Gomes [1,a], C. Gotti [21,k], M. Grabalosa Gándara [5], R. Graciani Diaz [37], L.A. Granado Cardoso [39], E. Graugés [37], E. Graverini [41], G. Graziani [18], A. Grecu [30], P. Griffith [46], L. Grillo [12], O. Grünberg [65], B. Gui [60], E. Gushchin [34], Yu. Guz [36,39], T. Gys [39], T. Hadavizadeh [56], C. Hadjivasiliou [60], G. Haefeli [40], C. Haen [39], S.C. Haines [48], S. Hall [54], B. Hamilton [59], X. Han [12], S. Hansmann-Menzemer [12], N. Harnew [56], S.T. Harnew [47], J. Harrison [55], J. He [39], T. Head [40], A. Heister [9], K. Hennessy [53], P. Henrard [5], L. Henry [8], J.A. Hernando Morata [38], E. van Herwijnen [39],

M. Heß [65], A. Hicheur [2], D. Hill [56], M. Hoballah [5], C. Hombach [55], L. Hongming [40], W. Hulsbergen [42], T. Humair [54], M. Hushchyn [67], N. Hussain [56], D. Hutchcroft [53], M. Idzik [28], P. Ilten [57], R. Jacobsson [39], A. Jaeger [12], J. Jalocha [56], E. Jans [42], A. Jawahery [59], M. John [56], D. Johnson [39], C.R. Jones [48], C. Joram [39], B. Jost [39], N. Jurik [60], S. Kandybei [44], W. Kanso [6], M. Karacson [39], T.M. Karbach [39,†], S. Karodia [52], M. Kecke [12], M. Kelsey [60], I.R. Kenyon [46], M. Kenzie [39], T. Ketel [43], E. Khairullin [67], B. Khanji [21,39,k], C. Khurewathanakul [40], T. Kirn [9], S. Klaver [55], K. Klimaszewski [29], M. Kolpin [12], I. Komarov [40], R.F. Koopman [43], P. Koppenburg [42,39], M. Kozeiha [5], L. Kravchuk [34], K. Kreplin [12], M. Kreps [49], P. Krokovny [35], F. Kruse [10], W. Krzemien [29], W. Kucewicz [27,o], M. Kucharczyk [27], V. Kudryavtsev [35], A.K. Kuonen [40], K. Kurek [29], T. Kvaratskheliya [32], D. Lacarrere [39], G. Lafferty [55,39], A. Lai [16], D. Lambert [51], G. Lanfranchi [19], C. Langenbruch [49], B. Langhans [39], T. Latham [49], C. Lazzeroni [46], R. Le Gac [6], J. van Leerdam [42], J.-P. Lees [4], R. Lefèvre [5], A. Leflat [33,39], J. Lefrançois [7], E. Lemos Cid [38], O. Leroy [6], T. Lesiak [27], B. Leverington [12], Y. Li [7], T. Likhomanenko [67,66], R. Lindner [39], C. Linn [39], F. Lionetto [41], B. Liu [16], X. Liu [3], D. Loh [49], I. Longstaff [52], J.H. Lopes [2], D. Lucchesi [23,r], M. Lucio Martinez [38], H. Luo [51], A. Lupato [23], E. Luppi [17,g], O. Lupton [56], N. Lusardi [22], A. Lusiani [24], X. Lyu [62], F. Machefert [7], F. Maciuc [30], O. Maev [31], K. Maguire [55], S. Malde [56], A. Malinin [66], G. Manca [7], G. Mancinelli [6], P. Manning [60], A. Mapelli [39], J. Maratas [5], J.F. Marchand [4], U. Marconi [15], C. Marin Benito [37], P. Marino [24,t], J. Marks [12], G. Martellotti [26], M. Martin [6], M. Martinelli [40], D. Martinez Santos [38], F. Martinez Vidal [68], D. Martins Tostes [2], L.M. Massacrier [7], A. Massafferri [1], R. Matev [39], A. Mathad [49], Z. Mathe [39], C. Matteuzzi [21], A. Mauri [41], B. Maurin [40], A. Mazurov [46], M. McCann [54], J. McCarthy [46], A. McNab [55], R. McNulty [13], B. Meadows [58], F. Meier [10], M. Meissner [12], D. Melnychuk [29], M. Merk [42], A. Merli [22,u], E. Michielin [23], D.A. Milanes [64], M.-N. Minard [4], D.S. Mitzel [12], J. Molina Rodriguez [61], I.A. Monroy [64], S. Monteil [5], M. Morandin [23], P. Morawski [28], A. Mordà [6], M.J. Morello [24,t], J. Moron [28], A.B. Morris [51], R. Mountain [60], F. Muheim [51], D. Müller [55], J. Müller [10], K. Müller [41], V. Müller [10], M. Mussini [15], B. Muster [40], P. Naik [47], T. Nakada [40], R. Nandakumar [50], A. Nandi [56], I. Nasteva [2], M. Needham [51], N. Neri [22], S. Neubert [12], N. Neufeld [39], M. Neuner [12], A.D. Nguyen [40], C. Nguyen-Mau [40,q], V. Niess [5], S. Nieswand [9], R. Niet [10], N. Nikitin [33], T. Nikodem [12], A. Novoselov [36], D.P. O'Hanlon [49], A. Oblakowska-Mucha [28], V. Obraztsov [36], S. Ogilvy [52], O. Okhrimenko [45], R. Oldeman [16,48,f], C.J.G. Onderwater [69], B. Osorio Rodrigues [1], J.M. Otalora Goicochea [2], A. Otto [39], P. Owen [54], A. Oyanguren [68], A. Palano [14,d], F. Palombo [22,u], M. Palutan [19], J. Panman [39], A. Papanestis [50], M. Pappagallo [52], L.L. Pappalardo [17,g], C. Pappenheimer [58], W. Parker [59], C. Parkes [55], G. Passaleva [18], G.D. Patel [53], M. Patel [54], C. Patrignani [20,j], A. Pearce [55,50], A. Pellegrino [42], G. Penso [26,m], M. Pepe Altarelli [39], S. Perazzini [15,e], P. Perret [5], L. Pescatore [46], K. Petridis [47], A. Petrolini [20,j], M. Petruzzo [22], E. Picatoste Olloqui [37], B. Pietrzyk [4], M. Pikies [27], D. Pinci [26], A. Pistone [20], A. Piucci [12], S. Playfer [51], M. Plo Casasus [38], T. Poikela [39], F. Polci [8], A. Poluektov [49,35], I. Polyakov [32], E. Polycarpo [2], A. Popov [36], D. Popov [11,39], B. Popovici [30], C. Potterat [2], E. Price [47], J.D. Price [53], J. Prisciandaro [38], A. Pritchard [53], C. Prouve [47], V. Pugatch [45], A. Puig Navarro [40], G. Punzi [24,s], W. Qian [56], R. Quagliani [7,47], B. Rachwal [27], J.H. Rademacker [47], M. Rama [24], M. Ramos Pernas [38], M.S. Rangel [2], I. Raniuk [44], G. Raven [43], F. Redi [54], S. Reichert [55], A.C. dos Reis [1], V. Renaudin [7], S. Ricciardi [50], S. Richards [47], M. Rihl [39], K. Rinnert [53,39], V. Rives Molina [37], P. Robbe [7], A.B. Rodrigues [1], E. Rodrigues [55], J.A. Rodriguez Lopez [64], P. Rodriguez Perez [55], A. Rogozhnikov [67], S. Roiser [39], V. Romanovsky [36], A. Romero Vidal [38], J.W. Ronayne [13], M. Rotondo [23], T. Ruf [39], P. Ruiz Valls [68], J.J. Saborido Silva [38], N. Sagidova [31], B. Saitta [16,f], V. Salustino Guimaraes [2], C. Sanchez Mayordomo [68], B. Sanmartin Sedes [38], R. Santacesaria [26], C. Santamarina Rios [38], M. Santimaria [19], E. Santovetti [25,l], A. Sarti [19,m], C. Satriano [26,n], A. Satta [25], D.M. Saunders [47], D. Savrina [32,33], S. Schael [9], M. Schiller [39], H. Schindler [39], M. Schlupp [10], M. Schmelling [11], T. Schmelzer [10], B. Schmidt [39], O. Schneider [40], A. Schopper [39], M. Schubiger [40], M.-H. Schune [7], R. Schwemmer [39], B. Sciascia [19], A. Sciubba [26,m], A. Semennikov [32], A. Sergi [46], N. Serra [41], J. Serrano [6], L. Sestini [23], P. Seyfert [21], M. Shapkin [36], I. Shapoval [17,44,g], Y. Shcheglov [31], T. Shears [53], L. Shekhtman [35], V. Shevchenko [66], A. Shires [10], B.G. Siddi [17], R. Silva Coutinho [41], L. Silva de Oliveira [2], G. Simi [23,s], M. Sirendi [48], N. Skidmore [47], T. Skwarnicki [60], E. Smith [54], I.T. Smith [51], J. Smith [48], M. Smith [55], H. Snoek [42], M.D. Sokoloff [58], F.J.P. Soler [52], F. Soomro [40], D. Souza [47], B. Souza De Paula [2], B. Spaan [10], P. Spradlin [52], S. Sridharan [39], F. Stagni [39], M. Stahl [12], S. Stahl [39], S. Stefkova [54], O. Steinkamp [41], O. Stenyakin [36], S. Stevenson [56], S. Stoica [30], S. Stone [60], B. Storaci [41], S. Stracka [24,t],

M. Straticiuc [30], U. Straumann [41], L. Sun [58], W. Sutcliffe [54], K. Swientek [28], S. Swientek [10], V. Syropoulos [43], M. Szczekowski [29], T. Szumlak [28], S. T'Jampens [4], A. Tayduganov [6], T. Tekampe [10], G. Tellarini [17,g], F. Teubert [39], C. Thomas [56], E. Thomas [39], J. van Tilburg [42], V. Tisserand [4], M. Tobin [40], S. Tolk [43], L. Tomassetti [17,g], D. Tonelli [39], S. Topp-Joergensen [56], E. Tournefier [4], S. Tourneur [40], K. Trabelsi [40], M. Traill [52], M.T. Tran [40], M. Tresch [41], A. Trisovic [39], A. Tsaregorodtsev [6], P. Tsopelas [42], N. Tuning [42,39], A. Ukleja [29], A. Ustyuzhanin [67,66], U. Uwer [12], C. Vacca [16,39,f], V. Vagnoni [15], S. Valat [39], G. Valenti [15], A. Vallier [7], R. Vazquez Gomez [19], P. Vazquez Regueiro [38], C. Vázquez Sierra [38], S. Vecchi [17], M. van Veghel [42], J.J. Velthuis [47], M. Veltri [18,h], G. Veneziano [40], M. Vesterinen [12], B. Viaud [7], D. Vieira [2], M. Vieites Diaz [38], X. Vilasis-Cardona [37,p], V. Volkov [33], A. Vollhardt [41], D. Voong [47], A. Vorobyev [31], V. Vorobyev [35], C. Voß [65], J.A. de Vries [42], R. Waldi [65], C. Wallace [49], R. Wallace [13], J. Walsh [24], J. Wang [60], D.R. Ward [48], N.K. Watson [46], D. Websdale [54], A. Weiden [41], M. Whitehead [39], J. Wicht [49], G. Wilkinson [56,39], M. Wilkinson [60], M. Williams [39], M.P. Williams [46], M. Williams [57], T. Williams [46], F.F. Wilson [50], J. Wimberley [59], J. Wishahi [10], W. Wislicki [29], M. Witek [27], G. Wormser [7], S.A. Wotton [48], K. Wraight [52], S. Wright [48], K. Wyllie [39], Y. Xie [63], Z. Xu [40], Z. Yang [3], H. Yin [63], J. Yu [63], X. Yuan [35], O. Yushchenko [36], M. Zangoli [15], M. Zavertyaev [11,c], L. Zhang [3], Y. Zhang [3], A. Zhelezov [12], Y. Zheng [62], A. Zhokhov [32], L. Zhong [3], V. Zhukov [9], S. Zucchelli [15]

[1] *Centro Brasileiro de Pesquisas Físicas (CBPF), Rio de Janeiro, Brazil*
[2] *Universidade Federal do Rio de Janeiro (UFRJ), Rio de Janeiro, Brazil*
[3] *Center for High Energy Physics, Tsinghua University, Beijing, China*
[4] *LAPP, Université Savoie Mont-Blanc, CNRS/IN2P3, Annecy-Le-Vieux, France*
[5] *Clermont Université, Université Blaise Pascal, CNRS/IN2P3, LPC, Clermont-Ferrand, France*
[6] *CPPM, Aix-Marseille Université, CNRS/IN2P3, Marseille, France*
[7] *LAL, Université Paris-Sud, CNRS/IN2P3, Orsay, France*
[8] *LPNHE, Université Pierre et Marie Curie, Université Paris Diderot, CNRS/IN2P3, Paris, France*
[9] *I. Physikalisches Institut, RWTH Aachen University, Aachen, Germany*
[10] *Fakultät Physik, Technische Universität Dortmund, Dortmund, Germany*
[11] *Max-Planck-Institut für Kernphysik (MPIK), Heidelberg, Germany*
[12] *Physikalisches Institut, Ruprecht-Karls-Universität Heidelberg, Heidelberg, Germany*
[13] *School of Physics, University College Dublin, Dublin, Ireland*
[14] *Sezione INFN di Bari, Bari, Italy*
[15] *Sezione INFN di Bologna, Bologna, Italy*
[16] *Sezione INFN di Cagliari, Cagliari, Italy*
[17] *Sezione INFN di Ferrara, Ferrara, Italy*
[18] *Sezione INFN di Firenze, Firenze, Italy*
[19] *Laboratori Nazionali dell'INFN di Frascati, Frascati, Italy*
[20] *Sezione INFN di Genova, Genova, Italy*
[21] *Sezione INFN di Milano Bicocca, Milano, Italy*
[22] *Sezione INFN di Milano, Milano, Italy*
[23] *Sezione INFN di Padova, Padova, Italy*
[24] *Sezione INFN di Pisa, Pisa, Italy*
[25] *Sezione INFN di Roma Tor Vergata, Roma, Italy*
[26] *Sezione INFN di Roma La Sapienza, Roma, Italy*
[27] *Henryk Niewodniczanski Institute of Nuclear Physics Polish Academy of Sciences, Kraków, Poland*
[28] *AGH – University of Science and Technology, Faculty of Physics and Applied Computer Science, Kraków, Poland*
[29] *National Center for Nuclear Research (NCBJ), Warsaw, Poland*
[30] *Horia Hulubei National Institute of Physics and Nuclear Engineering, Bucharest-Magurele, Romania*
[31] *Petersburg Nuclear Physics Institute (PNPI), Gatchina, Russia*
[32] *Institute of Theoretical and Experimental Physics (ITEP), Moscow, Russia*
[33] *Institute of Nuclear Physics, Moscow State University (SINP MSU), Moscow, Russia*
[34] *Institute for Nuclear Research of the Russian Academy of Sciences (INR RAN), Moscow, Russia*
[35] *Budker Institute of Nuclear Physics (SB RAS) and Novosibirsk State University, Novosibirsk, Russia*
[36] *Institute for High Energy Physics (IHEP), Protvino, Russia*
[37] *Universitat de Barcelona, Barcelona, Spain*
[38] *Universidad de Santiago de Compostela, Santiago de Compostela, Spain*
[39] *European Organization for Nuclear Research (CERN), Geneva, Switzerland*
[40] *Ecole Polytechnique Fédérale de Lausanne (EPFL), Lausanne, Switzerland*
[41] *Physik-Institut, Universität Zürich, Zürich, Switzerland*
[42] *Nikhef National Institute for Subatomic Physics, Amsterdam, The Netherlands*
[43] *Nikhef National Institute for Subatomic Physics and VU University Amsterdam, Amsterdam, The Netherlands*
[44] *NSC Kharkiv Institute of Physics and Technology (NSC KIPT), Kharkiv, Ukraine*
[45] *Institute for Nuclear Research of the National Academy of Sciences (KINR), Kyiv, Ukraine*
[46] *University of Birmingham, Birmingham, United Kingdom*
[47] *H.H. Wills Physics Laboratory, University of Bristol, Bristol, United Kingdom*
[48] *Cavendish Laboratory, University of Cambridge, Cambridge, United Kingdom*
[49] *Department of Physics, University of Warwick, Coventry, United Kingdom*
[50] *STFC Rutherford Appleton Laboratory, Didcot, United Kingdom*
[51] *School of Physics and Astronomy, University of Edinburgh, Edinburgh, United Kingdom*
[52] *School of Physics and Astronomy, University of Glasgow, Glasgow, United Kingdom*
[53] *Oliver Lodge Laboratory, University of Liverpool, Liverpool, United Kingdom*
[54] *Imperial College London, London, United Kingdom*

[55] School of Physics and Astronomy, University of Manchester, Manchester, United Kingdom
[56] Department of Physics, University of Oxford, Oxford, United Kingdom
[57] Massachusetts Institute of Technology, Cambridge, MA, United States
[58] University of Cincinnati, Cincinnati, OH, United States
[59] University of Maryland, College Park, MD, United States
[60] Syracuse University, Syracuse, NY, United States
[61] Pontifícia Universidade Católica do Rio de Janeiro (PUC-Rio), Rio de Janeiro, Brazil [v]
[62] University of Chinese Academy of Sciences, Beijing, China [w]
[63] Institute of Particle Physics, Central China Normal University, Wuhan, Hubei, China [w]
[64] Departamento de Fisica, Universidad Nacional de Colombia, Bogota, Colombia [x]
[65] Institut für Physik, Universität Rostock, Rostock, Germany [y]
[66] National Research Centre Kurchatov Institute, Moscow, Russia [z]
[67] Yandex School of Data Analysis, Moscow, Russia [z]
[68] Instituto de Fisica Corpuscular (IFIC), Universitat de Valencia-CSIC, Valencia, Spain [aa]
[69] Van Swinderen Institute, University of Groningen, Groningen, The Netherlands [ab]

* Corresponding author.
E-mail address: sean.benson@cern.ch (S. Benson).
[a] Universidade Federal do Triângulo Mineiro (UFTM), Uberaba-MG, Brazil.
[b] Laboratoire Leprince-Ringuet, Palaiseau, France.
[c] P.N. Lebedev Physical Institute, Russian Academy of Science (LPI RAS), Moscow, Russia.
[d] Università di Bari, Bari, Italy.
[e] Università di Bologna, Bologna, Italy.
[f] Università di Cagliari, Cagliari, Italy.
[g] Università di Ferrara, Ferrara, Italy.
[h] Università di Urbino, Urbino, Italy.
[i] Università di Modena e Reggio Emilia, Modena, Italy.
[j] Università di Genova, Genova, Italy.
[k] Università di Milano Bicocca, Milano, Italy.
[l] Università di Roma Tor Vergata, Roma, Italy.
[m] Università di Roma La Sapienza, Roma, Italy.
[n] Università della Basilicata, Potenza, Italy.
[o] AGH – University of Science and Technology, Faculty of Computer Science, Electronics and Telecommunications, Kraków, Poland.
[p] LIFAELS, La Salle, Universitat Ramon Llull, Barcelona, Spain.
[q] Hanoi University of Science, Hanoi, Viet Nam.
[r] Università di Padova, Padova, Italy.
[s] Università di Pisa, Pisa, Italy.
[t] Scuola Normale Superiore, Pisa, Italy.
[u] Università degli Studi di Milano, Milano, Italy.
[v] Associated to Universidade Federal do Rio de Janeiro (UFRJ), Rio de Janeiro, Brazil.
[w] Associated to Center for High Energy Physics, Tsinghua University, Beijing, China.
[x] Associated to LPNHE, Université Pierre et Marie Curie, Université Paris Diderot, CNRS/IN2P3, Paris, France.
[y] Associated to Physikalisches Institut, Ruprecht-Karls-Universität Heidelberg, Heidelberg, Germany.
[z] Associated to Institute of Theoretical and Experimental Physics (ITEP), Moscow, Russia.
[aa] Associated to Universitat de Barcelona, Barcelona, Spain.
[ab] Associated to Nikhef National Institute for Subatomic Physics, Amsterdam, The Netherlands.
† Deceased.